http://dx.doi.org/10.5012/bkcs.2014.35.11.3331

Mesoporous Carbon Additives for Long Cycle Life Sulfur Cathodes of Li-S Batteries

Jeong Yoon Koh, Tae Jeong Kim, Min-Sik Park,[†] Eun Hee Kim, Seok Kim,[‡] Ki Jae Kim,[†] Ji-Sang Yu,[†] Young-Jun Kim,[†,*] and Yongju Jung[*]

Department of Chemical Engineering, Korea University of Technology and Education (KOREATECH), Cheonan 330-708, Korea. [*]E-mail: yjung@koreatech.ac.kr
[†]Advanced Batteries Research Center, Korea Electronics Technology Institute, Seongnam 463-816, Korea [*]E-mail: yjkim@keti.re.kr
[‡]Department of Chemical Engineering, Pusan National University, Pusan 609-735, Korea
Received July 7, 2014, Accepted July 31, 2014

We examine the potential use of disordered mesoporous carbon as a functional additive for confining dissolved Li-polysulfides and improving the cycling performance of Li-S batteries. To promote a better understanding of the correlation between the total pore volume of disordered mesoporous carbon and the cycling performance of Li-S batteries, a series of disordered mesoporous carbons with different total pore volumes are successfully synthesized using a commercial silica template. Based on the electrochemical and structural analyses, we suggest that the total pore volume of disordered mesoporous carbon is a predominant factor in determining its capability for either the absorption or adsorption of Li-polysulfides, which is primarily responsible for enhancing the cycling performance. The addition of disordered mesoporous carbon is also effective in enhancing the homogeneous distribution of active sulfur in the cathode, thereby affecting the cycling performance.

Key Words : Mesoporous carbon additives, Li-S batteries, Cycling performance, Homogeneous distribution

Introduction

Lithium-sulfur (Li-S) batteries have been extensively explored as promising energy storage systems for electric vehicles and grid-supporting applications due to their high energy density and low cost.[1-3] Considerable efforts have been devoted to improving the practically available energy density of Li-S batteries, as well as to meeting the requirements for their commercial use. However, the cycling performance and rate-capability of currently available Li-S batteries need to be further improved before successful deployment on a commercial scale.[4-7]

To address such limitations, a robust design and facile synthesis of cathode materials are essential. Since Nazar *et al.* proposed the use of CMK-3, a typical mesoporous carbon, as a conducting framework,[8] tremendous attention has been directed towards developing robust sulfur composites using various conducting materials.[9-14] In particular, sulfur composites with mesoporous carbons have the greatest potential to effectively enhance the cycling performance of Li-S batteries.[15-17] It has been suggested that dissolved Li-polysulfides could be effectively confined within the mesopores of the integrated mesoporous carbon framework during cycling, thereby reducing the loss of active sulfur species while increasing sulfur utilisation.[18-20] Additionally, it has been proposed that the mesoporous carbon-based sulfur composites would offer several benefits: i) expanding the effective contact area of active sulfur; ii) securing the electrolyte pathway and electronic conduction; and iii) enhancing the mechanical stability of cathodes during cycling.[21-23] Despite the aforementioned advantages, an enhancement in the cycling performance of Li-S batteries through the application of mesoporous carbons to sulfur cathodes has not been fully elucidated. To create a better understanding of the role of mesoporous carbon in sulfur cathodes, the significance of the presence of mesoporous carbon in the cathode needs to be clarified. Moreover, the correlation between the structural characteristics of mesoporous carbon and the resultant electrochemical performance of Li-S batteries must be investigated.

To comprehensively understand the fundamental aspects, we investigated herein the effects of the total pore volume of mesoporous carbon on the cycling performance and the rate capability of Li-S batteries. We successfully synthesized disordered mesoporous carbon (DMC) samples with different total pore volumes and demonstrated their influence on the electrochemical performance of Li-S batteries when separately employed as additives in sulfur cathodes. The use of sulfur composites composed of mesoporous carbon additives and elemental sulfur is still challenging in terms of cost and mass production because the current synthetic process of mesoporous carbon-sulfur composites is cumbersome and poorly reproducible. Herein, we recommend the simple addition of mesoporous carbon into the sulfur cathode to allow an enhancement in the cycling performance of Li-S batteries. The results of this work will provide helpful insights for the design of robust S cathodes and for the development of advanced Li-S batteries.

Experimental

A series of DMC samples with different pore volumes

were designed and synthesized using a templating method with commercial colloidal silica templates (20 nm). For the synthesis of DMC, 6.5 g of sucrose ($C_{12}H_{22}O_{11}$, 99%, Junsei) was dissolved in de-ionized water and was thoroughly mixed with a colloidal silica solution (40% in H_2O, Alfa Aesar). To allow the formation of different pore volumes in the DMC, the ratios of silica to sucrose were varied over the range of 0.11 to 1.76. The mixtures were dried at 100 °C for 6 h and then at 160 °C for another 6 h to remove the residual solvent. After carbonization at 900 °C for 3 h under an N_2 atmosphere, the resultant solids were chemically etched with a 10% hydrofluoric (HF) acid solution to remove the silica templates, as described previously.[26] A micron-sized carbon material (the ratio of silica to sucrose = 0.11) was synthesized in the same process except for the HF etching. The carbon sample filled with silica template, denoted as non-porous DMC, was used for a control experiment. The final products were washed with de-ionized water repeatedly and dried at 100 °C before use.

The morphologies and microstructures of a series of DMC samples with different pore volumes were examined using field-emission scanning electron microscopy (FESEM, JEOL JSM-7000F) and high-resolution transmission electron microscopy (HRTEM, JEOL JEM3010). The surface area and the total pore volume of the DMC samples were measured using the Brunauer-Emmett-Teller (BET) and Barrett-Joyner-Halenda (BJH) methods by employing a surface area and porosimetry analyser (Tristar II 3020, Micromeritics). The removal of silica templates was confirmed using a thermogravimetric analyser (TGA, PerkinElmer TG/DTA 6300). The complete removal of the silica templates from the DMC was confirmed using TGA analysis (Figure S1).

A slurry composed of sulfur powder (60 wt %), a conducting agent (Ketjenblack, 10 wt %), DMC (10 wt %), and a binder (polyethylene oxide, 20 wt %) dissolved in acetonitrile was thoroughly mixed and coated on Al foil for cathode fabrication. For the electrochemical measurements, 2016 coin-type cells were assembled with the fabricated cathode (2.01 cm^2) and a lithium metal anode (2.54 cm^2) in an Ar-filled glove box. An electrolyte composed of 1.0 M lithium bis(trifluoromethanesulfonyl)imide (LiTFSI) dissolved in a mixture of dimethyl ether (DME), diglyme (DG), and 1,3-dioxolane (DOL) in a volumetric ratio of 6:2:2, including 0.3 M $LiNO_3$ as an additive, were used. The cells were discharged at various current densities of 0.05 C, 0.1 C, 0.25 C, 0.5 C, 1.0 C, and 1.5 C (1 C = 1674 mA/g) with a fixed charging current density of 0.1 C over a voltage range of 1.8 to 2.7 V *vs.* Li/Li^+ to examine the rate capability. The cycling tests were also conducted using a current density of 0.25 C during an additional 50 cycles just after the initial two cycles at 0.1 C.

Results and Discussion

To verify the effect of the simple addition of DMC to the sulfur cathode on the cycling performance and rate capability of Li-S batteries, we synthesized various DMC samples with different total pore volumes. The total pore volume of DMC was systematically controlled by adjusting the amount of colloidal silica during the synthesis. Figure 1 shows the FESEM images of a series of DMC samples synthesized using various ratios of silica to sucrose, including 0.11, 0.22, 0.44, 0.88, 1.32, and 1.76. As shown in Figure 1(a), DMC-0.11, synthesized using silica and sucrose in a ratio of 0.11, exhibits a relatively small number of mesopores, wherein the mesopores are sparsely formed on the surface of the carbon matrix. As expected, the sequential growth of the mesopore population was obvious as the ratio increased from 0.11 to 1.76. In the case of DMC-1.76, abundant mesopores were closely packed in the carbon matrix as a result of the deployment of the largest amount of silica template (Figure 1(f)). This finding revealed that the total pore volume of DMC was proportional to the quantity of incorporated silica template and was hence easily controllable in the proposed synthesis.

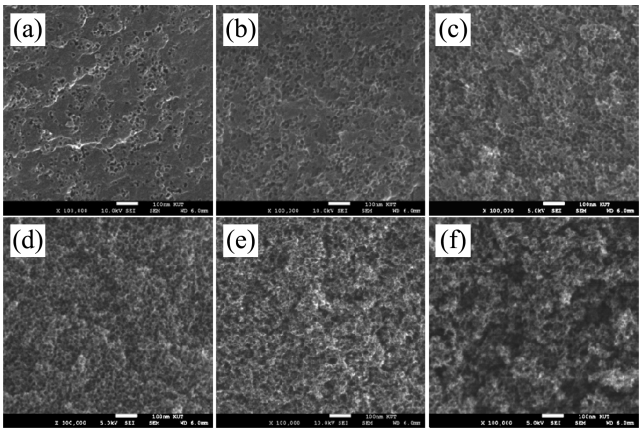

Figure 1. FESEM images of a series of DMC samples prepared using different ratios of silica to sucrose, such as (a) 0.11, (b) 0.22, (c) 0.44, (d) 0.88, (e) 1.32, and (f) 1.76, at the same magnification. All DMC samples were carefully etched with hydrofluoric acid to remove the silica templates. Note that (c) and (d) are FESEM images reported in the previous paper.[26]

The microstructures of the synthesized DMC samples were further confirmed using HRTEM observations. The DMC showed a highly porous structure in which abundant mesopores were successfully introduced into the amorphous carbon matrix. The pore population in the DMC grew with the increasing ratio of silica to sucrose (Figure 2), which was consistent with the FESEM observations. According to the HRTEM images in Figure 2, the mesopores and the thin amorphous carbon wall were well developed when the ratio of silica to sucrose is below 1.32. The pore size was in agreement with that of the silica template (~20 nm), and most of the mesopores were randomly distributed and separated from each other. In contrast, DMC-1.76 (Figure 2(f)) showed a distinctive microstructure in which some mesopores were partially broken and/or merged, thereby forming larger mesopores. This finding can be reasonably explained by the poor degree of dispersion of the nanoscale silica template when an excess amount of silica template was added during the synthesis.

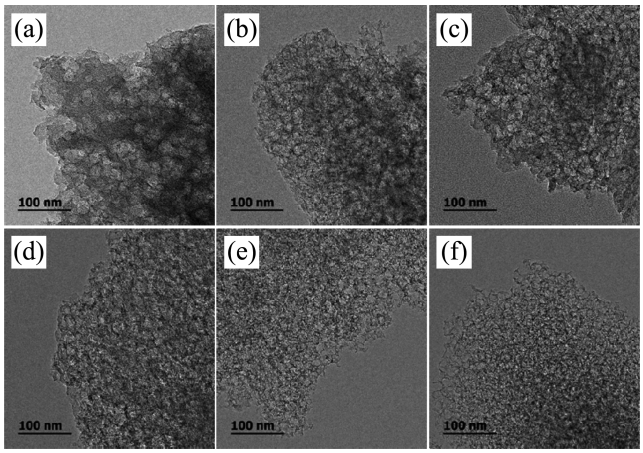

Figure 2. HRTEM images for the series of DMC after the removal of the silica templates using a 10% HF solution; (a) DMC-0.11 (b) DMC-0.22, (c) DMC-0.44, (d) DMC-0.88, (e) DMC-1.32, and (f) DMC-1.76.

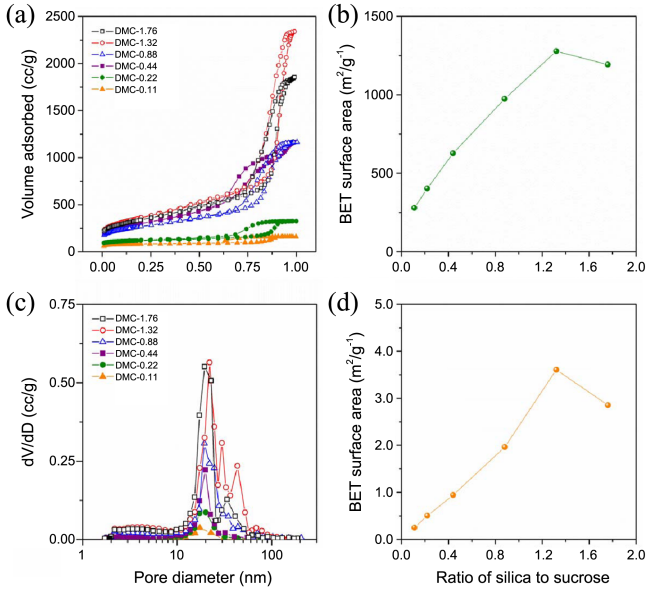

Figure 3. (a) N_2 isotherms and (b) BET surface areas, (c) pore size distributions, and (d) total pore volumes of a series of DMC samples with different ratios of silica to sucrose, such as 0.11 (△), 0.22 (○), 0.44 (□), 0.88(▲), 1.32 (●), and 1.76 (■). Note that N_2 isotherm results for DMC-0.44 and DMC-0.88 were reported previously.[26]

Figure 3 shows the N_2 isotherms and the pore size distributions of the DMCs synthesised using different ratios of silica to sucrose. All of the DMC samples showed typical N_2 adsorption-desorption curves with a hysteresis loop characteristic of mesoporous materials at high relative pressure (P/P_0), as shown in Figure 3(a).[24,25] The N_2 isotherms also allowed for the calculation of the BET surface areas of the DMC (Table 1). The surface area of DMC increased from 278 m^2/g (DMC-0.11) to 1277 m^2/g (DMC-1.32) with the increasing ratio of silica to sucrose (Figure 3(b)). However, DMC-1.76, prepared with an excess addition of silica template, led to a small reduction in the surface area (1192 m^2/g) compared to DMC-1.32. Figure 3(c) shows the pore size distributions of DMC calculated from the adsorption branches of the N_2 isotherm using the BJH method (Table 1). All DMC samples showed a pore size of approximately 20 nm, which was in accordance with the size of the silica template, as confirmed through the HRTEM observations. Analogous to the surface area, the total pore volume of DMC also showed a linear dependence on the quantity of silica template (Figure 3(d)). When the ratio of silica to sucrose increased from 0.11 to 1.32, a notable increase in the total pore volume of DMC was observed from 0.25 to 3.61 cc/g.

With an excess of silica (DMC-1.76), the total pore volume also decreased to 2.85 cc/g. A reduction in both the surface area and the total pore volume of DMC-1.76 was consistent with our observations obtained using electronic microscopes. When the quantity of silica exceeded a certain threshold, some mesopores were likely interconnected, which was responsible for the change in the microstructures of DMC.

The electrochemical performance of Li-S batteries was evaluated to clarify the effects of DMC addition. The rate capability of Li-S batteries, which is regarded as one of the most challenging aspects, was examined at different discharge currents of 0.05 C, 0.1 C, 0.25 C, 0.5 C, 1.0 C, and 1.5 C (1 C = 1674 mA/g). Figure 4(a) and 4(b) show the charge and discharge profiles of the cells with DMC-0.11 and DMC-1.32 at different current densities. The cell containing 10 wt % DMC-1.32 exhibited a reversible capacity of 1184.9 mAh/g in the first cycle with an initial coulombic efficiency of 88.2% at a current density of 0.05 C, which were better values compared to those obtained for the cell with DMC-0.11. The initial coulombic efficiency was estimated using the second discharge capacity *vs.* the first charge capacity. The cells with other types of DMC showed similar first discharge capacities; however, higher initial coulombic efficiencies were attained when the total pore volume of the DMC increased (Figure S2).

There was a noticeable difference in the charge and discharge profiles induced by different total pore volumes of

Table 1. BET surface area and total pore volume of a series of DMC samples after chemical etching with hydrofluoric acid. Note that data for DMC-0.44 and DMC-0.88 are reported previously[26]

	DMC-0.11	DMC-0.22	DMC-0.44	DMC-0.88	DMC-1.32	DMC-1.76
Ratio of Silica to Sucrose	0.11	0.22	0.44	0.88	1.32	1.76
Surface Area (m^2/g)	278.6	402.5	626.8	974.2	1277.5	1192.4
Pore Volume (cc/g)	0.25	0.51	0.94	1.96	3.61	2.85

DMC from the second cycle. The cell with DMC-1.32 showed the highest reversible capacity of 1045.1 mAh/g at the second cycle, compared to 701.8 mAh/g for the cell containing DMC-0.11. Such an undesirable capacity loss at the second cycle was mainly due to Li-polysulfide dissolution, and it was postulated that the mesopores of DMC were able to effectively trap the dissolved Li-polysulfides, thereby preventing the capacity loss. As expected, the capacity loss was significantly mitigated when the total pore volume of DMC increased. The amount of absorbed and/or trapped Li-polysulfides was highly dependent on the total pore volume of the DMC. This finding demonstrates that the total pore volume of the DMC was a predominant factor for a long cycle life of sulfur cathodes by trapping the dissolved Li-polysulfides. On the other hand, an improvement in the capacity retention due to the integration of DMC was obvious even at high current densities, such as 1.5 C. Based on these results, we found that the rate-capability of Li-S batteries could be slightly enhanced by the integration of DMC. The incorporated DMC additives provided more effective electric conduction and secured electrolyte pathways, leading to better Li^+ transport.

A higher correlation between the cycling performance and the total pore volume of DMC was also found. Figure 4(c) shows a comparison of the cycling performance of Li-S batteries employing the cathodes with various types of DMC.

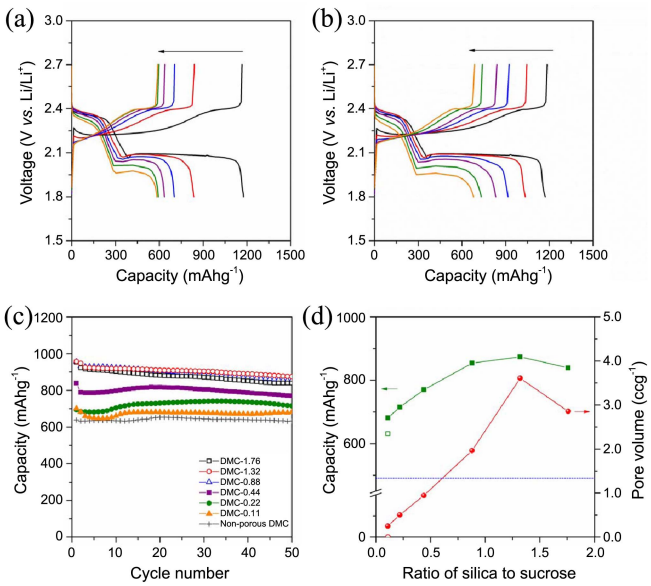

Figure 4. Rate capability of Li-S batteries containing 10 wt % of (a) DMC-0.11 and (b) DMC-1.32 in the cathodes; the cells were sequentially tested at different current densities of 0.05 C, 0.1 C, 0.25 C, 0.5 C, 1.0 C, and 1.5 C (1C = 1674 mA/g). (c) Cycling performance of sulfur cathodes containing 10 wt % DMC or non-porous DMC at a fixed current density of 0.25 C. Note that the electrochemical data for DMC-0.44 and DMC-0.88 were reported previously.[26] (d) Retention capacity of sulfur cathodes containing 10 wt % DMC (solid symbols) or non-porous DMC (open symbol) after 50 cycles as a function of the total pore volume of the DMC. The dotted line (···) indicates the retention capacity of a comparative cathode composed of 60 wt % elemental sulfur, 10 wt % Ketjenblack, and 30 wt % polyethyleneoxide.[26]

By utilizing DMC as a soluble Li-polysulfide reservoir in the cathodes, the capacity retention of the Li-S batteries was notably improved over 50 cycles. The cell containing DMC-1.32 exhibited a reversible capacity of 957.6 mAh/g at the first cycle, and 91.2% of the initial capacity was still maintained after 50 cycles, which are higher values compared to those of other cells assembled using DMC with smaller total pore volumes. The cycling performance of Li-S batteries was also closely related to the total pore volume of DMC. The high correlation was attributed to either the absorption or adsorption of Li-polysulfides by DMC.

Figure 4(d) plots the capacity retentions of Li-S batteries obtained after 50 cycles as a function of the total pore volume of DMC. The capacity retention increased proportionally to the total pore volume of the DMC. However, the retention capacity reached a saturated value when the total pore volume of DMC was higher than 2.0 cc/g. This finding could be due to the limited quantity of Li-polysulfides absorbed and/or trapped in the mesopores of the DMC. On the other hand, we found an improvement in the cycling performance of Li-S batteries after the addition of non-porous DMC containing silica template before chemical etching. Although the non-porous DMC did not have mesopores for confining Li-polysulfides, the cycling performance of the sulfur cathode with the non-porous DMC was greatly enhanced compared to that of the comparative cathode composed of elemental sulfur, conducting agent, and binder (Figure 4(d)).[25]

This result implies that the reason for the enhancement of the cycling performance of Li-S batteries could not be solely attributed to either the confining or absorption of the dissolved Li-polysulfides in the mesopores of the integrated DMC (Figure S3). To investigate the reason for the improvement due to the addition of non-porous DMC, further structural

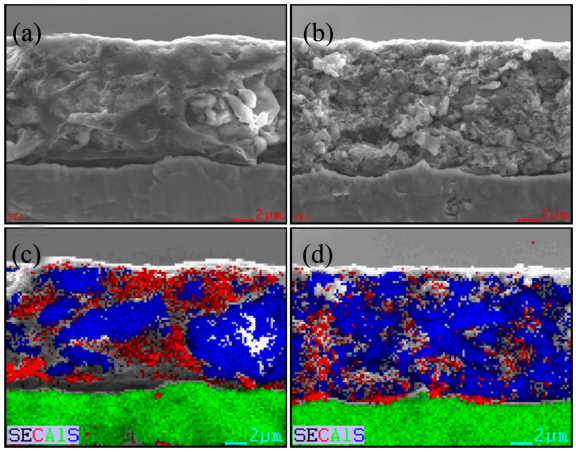

Figure 5. Cross-sectional FESEM images: (a) comparative cathode composed of 60 wt % elemental sulfur, 10 wt % Ketchen Black, and 30 wt % polyethyleneoxide and (b) cathode composed of 60 wt % elemental sulfur, 10 wt % Ketchen Black, 20 wt % polyethyleneoxide, and 10 wt % non-porous DMC before HF etching. The corresponding EDS results: (c) comparative cathode and (d) cathode with non-porous DMC without mesopores (sulfur: blue and carbon: red).

investigation was conducted for the cathode containing non-porous DMC before chemical etching in comparison with a micron-sized carbon particle-free cathode (comparative cathode).

Figure 5 shows the cross-sectional FESEM images combined with the EDS results for the cathode synthesized using non-porous DMC and the comparative cathode after the first cycle. As observed in Figure 5(a), significant structural collapses were observed in the comparative cathode, which originated from the dissolution and recombination of elemental sulfur during cycling. However, after the addition of non-porous DMC, the structural degradation was not as significant as the comparative cathode. The cathode containing non-porous DMC still maintained its porous structure and better elemental sulfur distribution compared to the comparative cathode (Figure 5(c) and 5(d)). Therefore, the addition of DMC enhanced the homogeneous distribution of active S in the cathodes. As a conducting framework, the DMC can support the cathode structure even after forming soluble Li-polysulfides during cycling. Importantly, the integration of DMC was effective in maintaining good S distribution as well as the porosity of the cathode during cycling, which were responsible for the improved performance of Li-S batteries. Thus, we determined the significance of DMC in the sulfur cathode by i) confining soluble Li-polysulfides during cycling and ii) enhancing homogeneous sulfur distribution in the cathode, which effectively promoted good cycling performance of Li-S batteries (Figure S4).

Conclusion

Based on the systematic variation of the total pore volume of DMC, we clearly demonstrated the correlation between the total pore volume of DMC and the electrochemical performance of Li-S batteries. The total pore volume of the DMC additive predominantly affected the cycling performance and rate-capability of Li-S batteries. The primary role of the DMC additive was to confine the soluble Li-polysulfides, which effectively minimized the capacity loss induced by dissolved Li-polysulfides. The addition of DMC was also effective in enhancing the structural stability of the cathodes. Even after the addition of non-porous DMC filled with silica template (micron-sized carbon material without mesopores), the cycling performance of the Li-S batteries improved, which indicated that securing the structural integrity of the cathode was also important for further enhancement of the performance. Our findings revealed a previously overlooked positive effect of mesoporous carbon on the electrochemical performance of Li-S batteries and demonstrated the significance of the critical design of the cathodes. We believe that these results should provide new insights for further improvement in the performance of Li-S batteries.

Acknowledgments. The authors thank the Technology Innovation Center, SK Holdings, for their financial support in the development of Li_xS_y solid-state batteries. This work was partially supported by the Energy Efficiency & Resources Core Technology Program of the Korea Institute of Energy Technology Evaluation and Planning (KETEP) granted financial resource from the Ministry of Trade, Industry & Energy, Republic of Korea (No. 20132020000260).

References

1. Bruce, P. G.; Freunberger, S. A.; Hardwick, L. J.; Tarascon, J. M. *Nat. Mater.* **2012**, *11,* 19.
2. Tarascon, J. M.; Armand, M. *Nature* **2001**, *414*, 359.
3. Bruce, P. G.; Scrosati, B.; Tarascon, J. M. *Angew. Chem. Int. Ed.* **2008**, *47*, 2930.
4. Jung, Y.; Kim, S. *Electrochem. Commun.* **2007**, *9*, 249.
5. Kim, S.; Jung, Y.; Park, S. J. *J. Power Sources* **2005**, *152*, 272.
6. Evers, S.; Nazar, L. F. *Acc. Chem. Res.* **2013**, *46*, 1135.
7. Manthiram, A.; Fu, Y. Z.; Su, Y. S. *Acc. Chem. Res.* **2013**, *46*, 1125.
8. Ji, X.; Lee, K. T.; Nazar, L. F. *Nat. Mater.* **2009**, *8*, 500.
9. Zheng, G.; Yang, Y.; Cha, J. J.; Hong, S. S.; Cui, Y. *Nano Lett.* **2011**, *11*, 4462.
10. Park, M. S.; Yu, J. S.; Kim, K. J.; Jeong, G.; Kim, J. H.; Jo, Y. N.; Hwang, U.; Kang, S.; Woo, T.; Kim, Y. J. *Phys. Chem. Chem. Phys.* **2012**, *14*, 6796.
11. Jayaprakash, N.; Shen, J.; Moganty, S. S.; Corona, A.; Archer, L. A. *Angew. Chem. Int. Ed.* **2011**, *50*, 5904.
12. Wang, H.; Yang, Y.; Liang, Y.; Robinson, J. T.; Li, Y.; Jackson, A.; Cui, Y.; Dai, H. *Nano Lett.* **2011**, *11*, 2644.
13. Rao, M.; Song, X.; Liao, H.; Cairns, E. J. *Electrochim. Acta* **2012**, *65*, 228.
14. Guo, J.; Xu, Y.; Wang, C. *Nano Lett.* **2011**, *11*, 4288.
15. Elazari, R.; Salitra, G.; Garsuch, A.; Panchenko, A.; Aurbach, D. *Adv. Mater.* **2011**, *23*, 5641.
16. Park, M. S.; Yu, J. S.; Kim, K. J.; Jeong, G.; Kim, J. H.; Yim, T.; Jo, Y. N.; Hwang, U.; Kang, S.; Woo, T.; Kim, H.; Kim, Y. J. *RSC Adv.* **2013**, *3*, 11774.
17. Liang, C.; Dudney, N. J.; Howe, J. Y. *Chem. Mater.* **2009**, *21*, 4724.
18. Schuster, J.; He, G.; Mandlmeier, B.; Yim, T.; Lee, K. T.; Bein, T.; Nazar, L. F. *Angew. Chem. Int. Ed.* **2012**, *51*, 3591.
19. Seh, Z. W.; Li, W.; Cha, J. J.; Zheng, G.; Yang, Y.; McDowell, M. T.; Hsu, P. C.; Cui, Y. *Nat. Commun.* **2013**, *4*, 1331.
20. Ji, X.; Evers, S.; Black, R.; Nazar, L. F. *Nat. Commun.* **2011**, *2*, 325.
21. Lai, C.; Gao, X. P.; Zhang, B.; Yan, T. Y.; Zhou, Z. *J. Phys. Chem. C* **2009**, *113*, 4712.
22. Shim, J.; Striebel, K. A.; Cairns, E. J. *J. Electrochem. Soc.* **2002**, *149*, A1321.
23. Li, X.; Cao, Y.; Qi, W.; Saraf, L. V.; Xiao, J.; Nie, Z.; Mietek, J.; Zhang, J. G.; Schwenzer, B.; Liu, J. *J. Mater. Chem.* **2011**, *21*, 16603.
24. Kruk, M.; Jaroniec, M.; Sayari, A. *Langmuir* **1997**, *13*, 6267.
25. Kruk, M.; Jaroniec, M. *J. Phys. Chem. B* **2002**, *106*, 4732.
26. Park, M. S.; Jeong, B. O.; Kim, T. J.; Kim, S.; Kim, K. J.; Yu, J. S.; Jung, Y.; Kim, Y. J. *Carbon* **2014**, *68*, 265.